# A SIMPLE ROUTE SYNTHESIS OF Cr-DOPED NiO NANOPARTICLES AND THEIR CHARACTERISATION STUDIES

## P. M. PONNUSAMY[*], S. AGILAN[a] and N. MUTHUKUMARASAMY[a]

Department of Physics, SNS College of Technology, COIMBATORE (T.N.) INDIA
[a]Department of Physics, Coimbatore Institute of Technology, COIMBATORE (T.N.) INDIA

## ABSTRACT

Nano scale NiO and Cr doped NiO nanoparticles (NPs) have been prepared by simple chemical co-precipitation method. The structure, morphology, band gap energy and magnetic properties of the synthesized samples have been examined by X-ray diffraction, SEM, HRTEM, UV absorption and VSM, respectively. The insertion of Cr ions into NiO NPs gives significant changes in structural and magnetic properties. The crystalline size of Cr-doped NiO was calculated and it is around 20 nm. The UV absorption study shows strong absorption peak around 300 nm. The magnetic property was studied using Vibrating Sample Magnetometer (VSM) and NiO NPs exhibit super paramagnetic behavior, which differs from bulk form whereas Cr-doped NiO NPs magnitization curve recorded the appearance of diamagnetic behaviour and was found suitable for spin value applications.

**Key words**: Chemical co-precipitation, NiO nanoparticles, Spin value, VSM, FESEM, HRTEM and UV-Visible.

## INTRODUCTION

Nano materials have received much attention in the exciting area of research because of significant electronic, optical and magnetic properties when compared to its bulk form[1,2]. NiO nanoparticles are p-type, wide band gap semiconductor, which is an important material used in high tech applications like smart windows, elecrochemical super capacitor and also in dye sensitized photocathode[3-8]. Anomalous magnetic behaviour was observed because of size effects and this fact has been due to the presence of larger value of surface atoms having uncompensated spins (higher magnetization value)[9,10]. NiO nanoparticles show super paramagnetic and super antiferromagnetic behaviour observed in the particles range from 13-18 nm[11].

_____

[*]Author for correspondence; E-mail: surya.ponnusamy@gmail.com; Mo.: +91-9942586302

In most of the magnetic applications, nanoparticles of specific grain size, morphology, uniform particle distribution and desire phase purity was needed. However, synthesing desired grain size without particle agglomation at room temperature was a challenging problem. The preparation of magnetic nanoparticles was very important for applications in spintronics devices. Several methods have been adopted to synthesis NiO nanoparticles such as sputtering, electron beam evaporation, solvothermal method, hydrothermal, sol-gel, infrared heating and thermal evaporation[12-17]. Among the various synthesis techniques, effective co-precipitation chemical route was used to synthesise NiO and Cr-doped NiO nanoparticles with controlled particle size. The present work discusses the effects of Cr-ion insertion to NiO nanoparticles on structural, grain size and magnetic property.

## EXPERIMENTAL

All the chemical reagents are commercially available analytical grade reagents and are used without further purification. Double distilled water was used throughout the experiments. NiO and Cr-doped NiO nanoparticles were prepared by co-precipitation method. To prepare nanoparticles, $Ni(NO_3)_2.6H_2O$ was dissolved in 100 mL of double distilled water (and chromium nitrate: $Cr(NO_3).9H_2O$ for Cr-doped samples) and stirred for 30 mins. After thorough stirring, 100 mL of NaOH was added drop by drop at room temperature and finally precipitate was obtained. The obtained precipitate at different mole ratio was centrifuged and then washed with double distilled water several times to remove the unwanted impurities. After that, the collected colloidal precipitate was allowed to dry in an oven at 70ºC for 12 hrs. The dried sample obtained was sintered at 350ºC for 2 hrs in a closed muffle furnace. They are labelled as NS1, NS2, NS3 and NS4 for 0.1 M, 0.2 M, 0.3 M and 0.4 M. Then 5%, 10% and 15% Cr-doped with NiO NPs samples are labelled as $NCr_1$, $NCr_2$ and $NCr_3$, respectively.

The structure and morphology of as prepared samples was characterized by XRD (XPERT-PRO PW3050) and electron microscopy analysis [FESEM (Zeiss) & HRTEM (JEOL JEM-2100F)]. The UV-Visible absorption spectra was recorded using spectrophotometer (JASCO V-570) in the range of 200-800 nm to determine the band gap of the prepared samples. Magnetic behaviour was recorded from a vibrating sample magnetometer (Lake Shore: Model: 7404).

## RESULTS AND DISCUSSION

The XRD pattern of the NiO nanoparticles prepared using different mole ratios are shown in Fig. 1. All the reflection peaks present at (111), (200), (220), (311) & (222) [JCPDS Card No.: 01-078-0423] corresponds to FCC structure of NiO nanoparticles. The

result clearly shows that the synthesised NiO nanoparticles had high purity with the absence of impurity peaks. Fig. 2 shows the XRD pattern of the NiO and Cr-doped NiO NPs, the addition of Cr-ion enhance the broadening of peak and the impurity phase was observed in Cr-doped NiO nanoparticles.
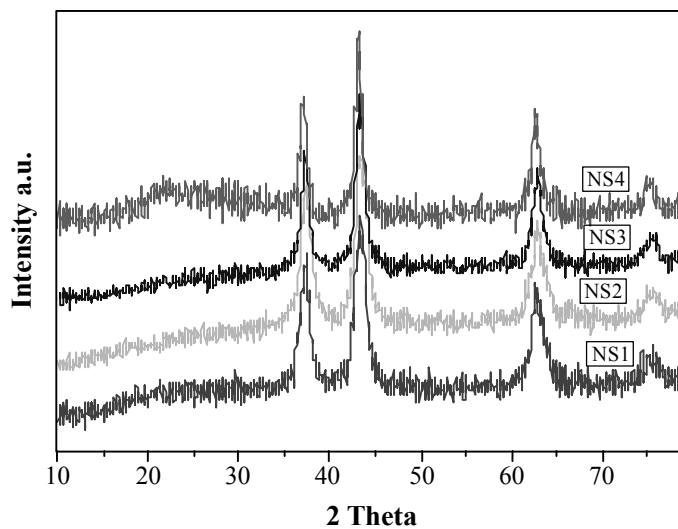


**Fig. 1: XRD pattern of NiO nanoparticles prepared using different molar concentrations**
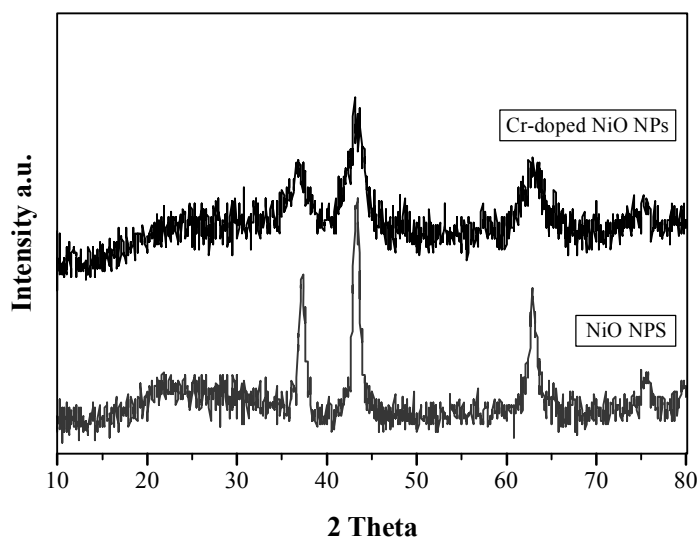


**Fig. 2: XRD pattern of NiO and Cr-doped NiO nanoparticles prepared using 0.1 M molar concentrations**

The crystallite size has been estimated by using the Scherer relation,

$$D = 0.916 \, \lambda / \beta \, Cos \, \theta \qquad \qquad …(1)$$

where D is the grain size, $\lambda$ is the X-ray wave length, $\beta$ is the full width at half maximum intensity and $\theta$ is the Bragg's angle and the calculated values was found to be 11.97, 10.33, 14.22 and 16.21 nm for NiO nanoparticles prepared with 0.1 M, 0.2 M, 0.3 M and 0.4 M concentrations. Similarly the crystallite sizes of Cr-doped NiO NPs are 9.61, 9.54 & 9.67 nm with 5%, 10% and 15% Cr concentrations. This shows that the doping of Cr ions reduces the grain size of NiO nanoparticles, the insertion of Cr ion on NiO creates internal micro strain and lattice parameter with reduced grain size[4]. The reduced grain size indicates that the growth of host lattice was restricted by Cr-ion. The microstructural disorder was due to the differences in the ionic radii of $Ni^{2+}$ (0.69 Å) and $Cr^{2+}$ ion (0.89Å). The crystallite sizes estimated from HRTEM analysis matches with the XRD results. Table 1 shows the particle size, d-spacing and band gap values of the prepared samples.

**Table 1: Particle size, d-spacing and band gap values of the prepared samples**

| Sample | Particle size (nm) | d-spacing (Å) (111) plane | Band gap (eV) |
|--------|--------------------|----------------------------|----------------|
| NS1    | 11.97              | 2.087                      | 4.02           |
| NS2    | 10.33              | 2.085                      | 4.06           |
| NS3    | 14.22              | 2.090                      | 4.07           |
| NS4    | 16.21              | 2.088                      | 4.07           |
| NCr1   | 9.61               | 2.061                      | 4.10           |
| NCr2   | 9.54               | 2.085                      | 4.19           |
| NCr3   | 9.67               | 2.072                      | 4.17           |

Fig. 3 shows the surface morphology and particle size distribution of NiO NPs. The image clearly shows that the particles are non-spherical, highly porous and the average particle size around 12 nm to 16 nm. The SEM images of Cr doped NiO NPs is shown in Fig. 4. The image clearly shows that the sample having uniform grain size with average particle size of 10 nm. The obtained values match with the XRD results.
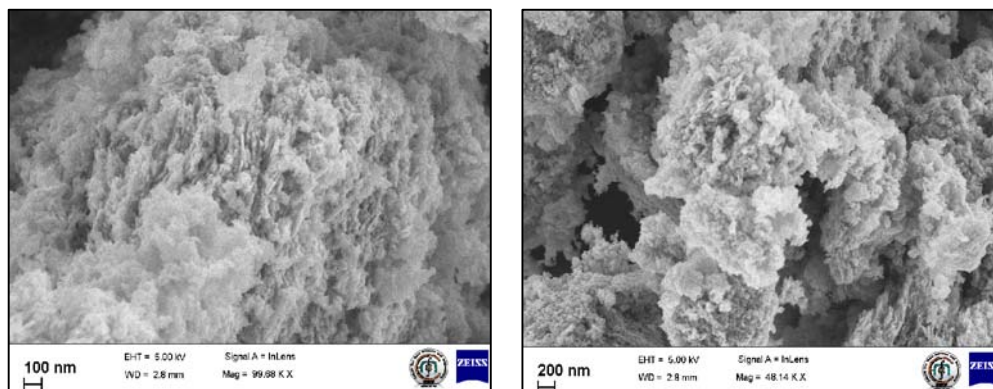
**Fig. 3: FESEM image of NiO NPs with different magnifications**
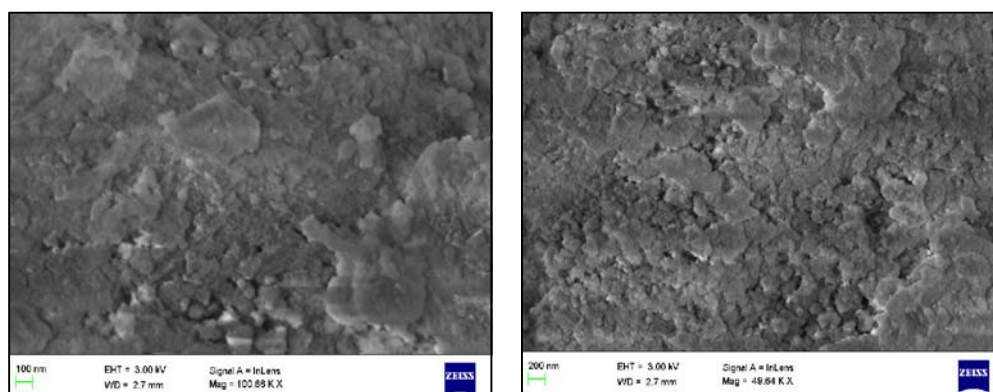


**Fig. 4: FESEM image of Cr-doped NiO NPs with different magnifications**

The insertion of Cr-ion on NiO reduces the grain size, which indicates the increase of strain in the matrix and restricts the lattice growth. The estimated grain size from HRTEM images shows appreciable agreement with XRD results. The HRTEM result helps to check out the crystallinity and phase purity of as prepared samples. Fringes of uniform width have been observed (Fig. 5) in HRTEM image reveals the high crystallinity and defect free nature of the sample. The d-spacing was calculated for (200) planes of NiO and Cr-doped NiO and the calculated values are 2.08 Å and 2.085 Å, respectively. Fig. 6 shows the selected area electron diffraction (SAED) pattern of NiO and Cr-doped NiO nanocrystals. The observed rings of the samples proved the crystalline nature and the pure form of NiO.
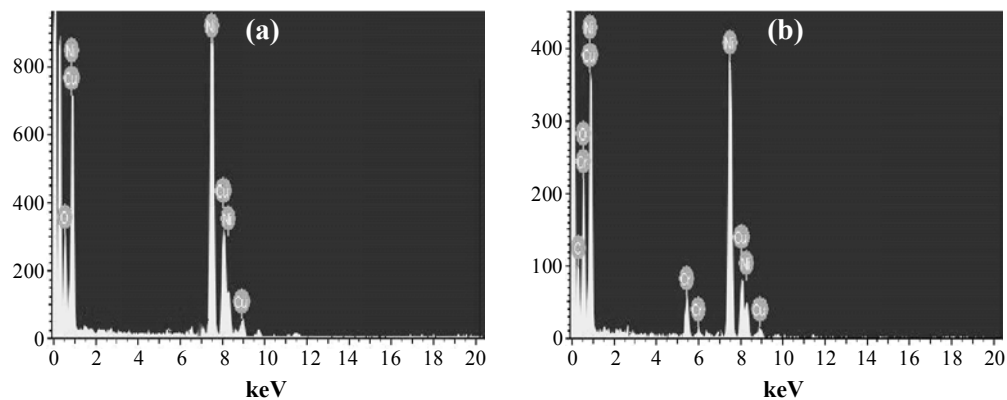
Fig. 7 (a,b) shows the EDS spectrum of NiO and Cr-doped NiO NPs, where Ni and O are the main components. The Cu peak in the figure originates from the grid used in TEM for EDS observation. From Fig. 7(b), the less percentage of Cr-ion incorporated in the sample clearly predicts the proper doping.
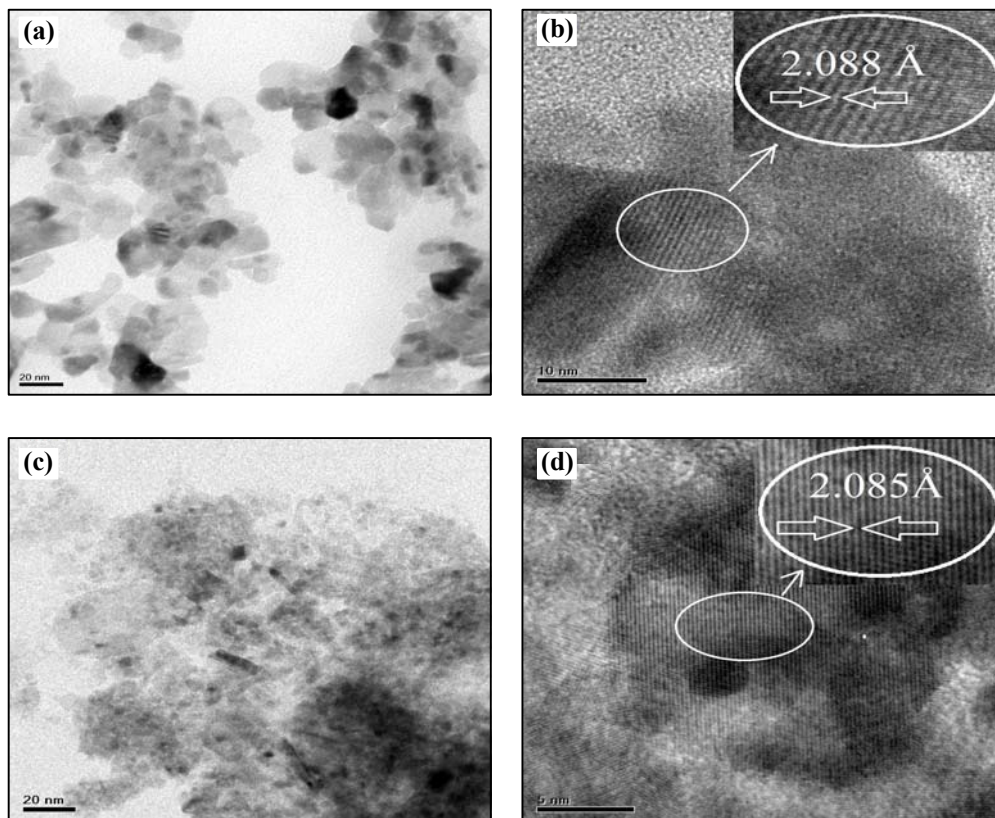
**Fig. 5: HR-TEM image of (a) NiO and (b) fringe pattern of NiO NPs (c) Cr-doped NiO and (d) fringe pattern of Cr-doped NiO NPs**
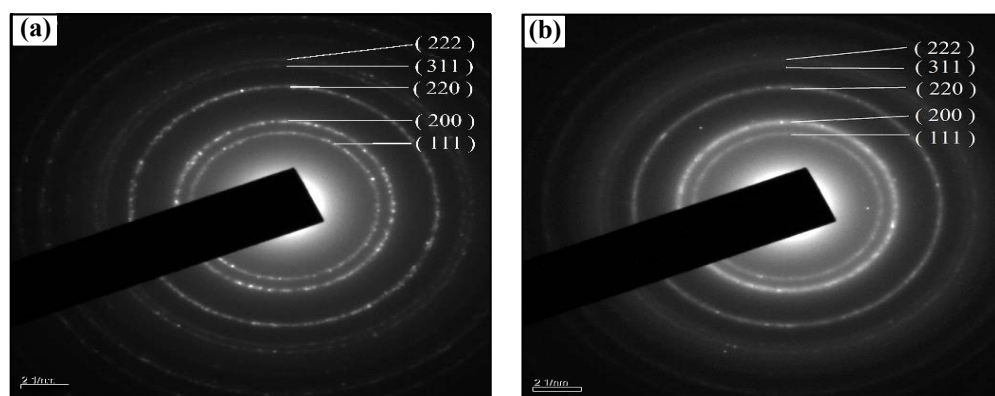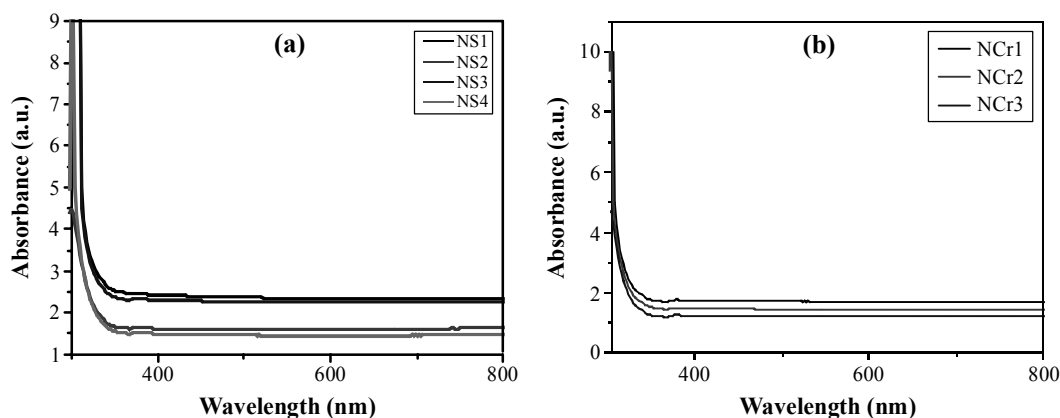


**Fig. 6: SAED Pattern of (a) NiO and (b) Cr-doped NiO NPs**

**Fig. 7: EDS spectrum of (a) NiO NPs and (b) Cr-doped NiO NPs**

Fig. 8 (a,b) shows the optical absorption spectrum of NiO NPs and Cr-doped NiO NPs, respectively. In both the cases absorption was shifted towards blue region and it is below 450 nm (2.76 eV). The absorption edge at 308, 305, 304, 304 and 296 nm for the samples NS1, NS2, NS3, NS4 and NCr.



**Fig. 8: Absorbance spectra of (a) NiO NPs and (b) Cr-doped NiO NPs**

This shift towards blue region indicates that there was an increase in band gap, which leads to the decrease in particle size. The absorption coefficient ($\alpha$) and the incident photon energy ($h\nu$) are related by the equation[18].

$$(\alpha h\nu) = A(h\nu - E_g)^n \qquad \ldots(2)$$

where A is a constant relative to materials, $E_g$ is the band gap of the material, $\nu$ is the frequency of the incident radiation, h is the Planck's constant and n is 1/2 for direct band

semiconductor and 2 for indirect band gap semiconductor. The optical band gap of the NiO NPs and Cr-doped NiO NPs have been determined using the equation 2. Fig. 9 (a,b) shows the $(\alpha h\nu)^2$ versus h$\nu$ plot of NiO NPs and Cr-doped NiO NPs with different molar and Cr-doping concentrations. The optical band gap values have been determined by extrapolating the linear portion of the the curve to meet the energy axis (h$\nu$). The band gap of NiO was found to be 4.02 to 4.07 eV and Cr-doped NiO NPs was around 4.10 to 4.19 eV. The band gap found to vary due to quantum confinement effect. The increase of $E_g$, which implies that the particle size became smaller.
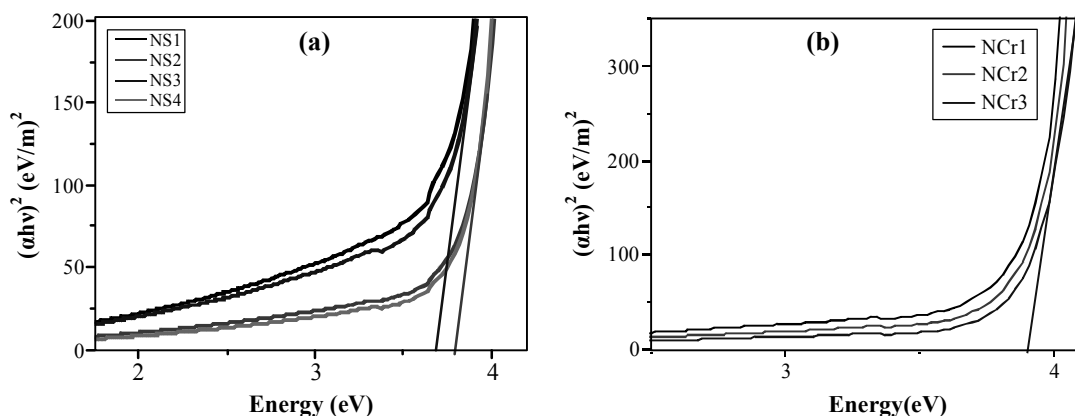


**Fig. 9: Plot of $(\alpha h\nu)^2$ vs. photon energy of (a) NiO NPs and (b) Cr-doped NiO NPs**

Fig. 10(a,b) shows the magnetic properties of samples analysed by vibrating sample magnetometer at room temperature. The magnetization versus applied magnetic field plots for the NiO NPs shows the existence of superparamagnetic behaviour whereas bulk NiO shows antiferromagnetism[19]. Magnetic NiO nanoparticles possess uncompensated spins due to the presence of more surface atoms and formation of magnetic clusters on the particles surface results in net magnetism. Smaller the crystallites size, more will be the net magnetization. The existences of magnetic property are very closely associated with fine grain microstructure of the particles. The Cr-doped NiO NPs show diamagnetic like behaviour due to the compensation of spin values. The narrowed hysteresis curves of Cr-doped NiO have low coercive field (Hc) and remanent magnetization ($M_R$) was due to the lattice imperfection, which causes the lowering of net magnetization. The occurrence of dia-magnetic features are related to superconducting phenomenon, which was observed in Cr-doped NiO NPs. These magnetic behaviour of the materials are widely used in the promising application of gas sensors and superconducting devices.
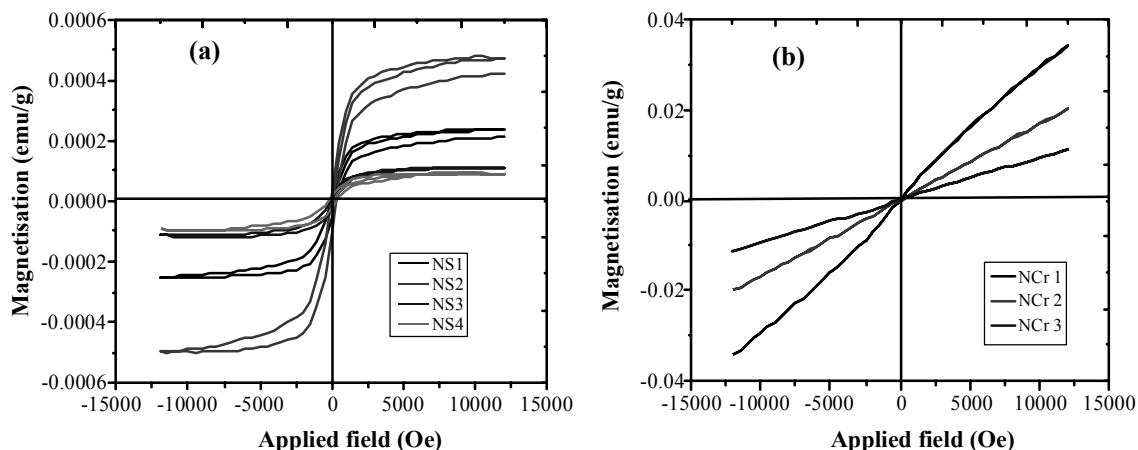
**Fig. 10: Hysteresis curves of (a) NiO NPs and (b) Cr-doped NiO NPs**

## CONCLUSION

NiO NPs and Cr-doped NiO NPs have been successfully prepared by Co-precipitation method. The XRD results confirmed the formation of NiO and Cr-doped NiO NPs. The insertion of Cr-ion reduces the particle size. The SEM and HRTEM helps to analysis the porous nature and d-spacing. Optical absorbance study reveals that the synthesized NPs exhibited the absorption peak around 300 nm and the band gap was determined to be around 4 eV. The VSM study shows the magnetic behaviour arise of uncompensated spin value and fine microstructure. This method was economic and high yield process which fulfils the demanding applications.

## REFERENCES

1. L. Neel, C. R. Acad. Sci., Paris, **228**, 664 (1949).

2. Hotovy, J. Huran, L. Specess, S. Hascik and Rehacek, Sensors and Actuators B., **57 (1-3)**, 147-152 (1999).

3. F. Reinert, P. Steiner, Hufner, H. Schmitt, J. Fink, M. Knupfer, P. Sandal and E. Bertel, Z. Phys. B., **97**, 83 (1995).

4. C. G. Granqvist, Handbook of Electrochromic Materials, Ed., Elsevier: Amsterdam (1995).

5. K. Liu and M. Anderson, J. Electrochem. Soc., **143**, 124 (1996).

6. V. Srinivasan and J. Weidner, J. Electrochem. Soc., **144**, L210 (1997).

7.   H. Y. Ryu, G. P. Choi, W. S. Lee and J. S. Park, J. Matter. Sci. Lett., **39**, 4375 (2004).

8.   J. He, H. Lindstrom, A. Hagfeldt and S. E. Lindquist, J. Phys. Chem. B., **103**, 8940 (1999).

9.   R. H. Kodama, S. A. Makhlouf and A. E. Berkowitz, Phys. Rev. Lett., **79**, 1393 (1997).

10.  E. Winkler, R. D. Zysler, M. Vasquez Mansilla and D. Fiorani, Phys. Rev. B., **72**, 132409 (2005).

11.  M. Abdul Khadar, V. Biju and A. Inoue, Mater. Res. Bull., **38**, 1341 (2003).

12.  D. Wruck and M. Rubin, J. Electrochem. Soc., **140**, 1097 (1993).

13.  S. Yamada, T. Yoshuoka, M. Miyashita, K. Urabe and M. Kiato, J. Appl. Phys., **63**, 2116 (1988).

14.  K. Yoshimura, T. Miki and S. Tanemura, Japan J. Appl. Phys., **34**, 2440 (1995).

15.  A. Surca, B. Orel, B. Pihlar and P. Bukovec, J. Electroanal. Chem., 40883 (1996).

16.  R. Cinnsealach, G. Boschloo, S. N. Rao and D. Fitzmaurice, Sol. Energy Matter. Sol. Cels., **57**, 107 (1999).

17.  A. Agrawal, H. R. Habibi, R. K. Agrawal, J. P. Cronin, D. M. Roberts, R. Caron-Popowich and C. M. Lampert, Thin Solid Films, **221**, 239-253 (1992).

18.  J. I. Pancove, Optical Processes in Semiconductors, Englewood Cliffs, NJ: Prentice Hall (1971).

19.  P. Ngo, P. Bonville and M. P Pileni. Nanoparticles of $Co_xFe_{y-z}O_4$: Synthesis and Superparamagnetic Properties, Eur. Phys. J. B., **9**, 583 (1999).